

Image Retrieval Using Fusion of Sauvola and Thepade's Sorted Block Truncation Coding-Based Color Features

Jaya H. Dewan¹ and Sudeep D. Thepade^{2*}

¹Department of Information Technology, Pimpri Chinchwad College of Engineering, Pune 411044, India

²Department of Computer Engineering, Pimpri Chinchwad College of Engineering, Pune 411044, India

ABSTRACT

Because of the tremendous growth in digital imaging, enhanced communication and storage technology, billions of images are captured, stored, and exchanged daily. Finding and searching for an image in a large collection is becoming challenging. The query by reference image retrieval (IR) technique aims to close the semantic gap between the query and retrieve images while improving performance. The primary goal of the work proposed here is to develop discriminative and descriptive features of the image with the minimum possible size. Here, the weighted feature fusion-based IR technique is proposed using Sauvola local thresholding (SLT) and Thepade's Sorted Block Truncation Coding (SBTC) methods. The proposed technique is tested using two standard datasets with mean square error (MSE) as a distance measure and average retrieval accuracy (ARA) as a performance metric. The technique has contributed to the enhancement of ARA with the small and fixed-size image feature vector. The feature vector generated is much smaller than the image dimension and is used as a feature vector to represent the image for retrieval. Results prove that the proposed technique of SBTC 8-ary with 0.1 weight and SLT with 0.9 weight feature fusion gives better ARA than other techniques studied.

Keywords: Color features, content-based image retrieval, Sauvola thresholding, Thepade's Sorted Block Truncation Coding (SBTC)

ARTICLE INFO

Article history:

Received: 27 May 2022

Accepted: 14 November 2022

Published: 13 July 2023

DOI: <https://doi.org/10.47836/pjst.31.5.06>

E-mail addresses:

jaya.h.dewan@gmail.com (Jaya H. Dewan)
sudeepthepade@gmail.com (Sudeep D. Thepade)

* Corresponding author

INTRODUCTION

People have been utilizing images to transmit thoughts and information to one another since prehistoric times using cave drawings. Images have long been regarded as necessary for communication, as images can easily catch attention, elicit emotions,

and transmit information quickly. Use of digital cameras, smartphones, and the Internet have increased due to technological imaging, networking, and storage advancements. The complexity and the amount of multimedia, especially image data generated, stored, transmitted, shared, analyzed, and accessed, is increasing enormously. However, this data is only useful if it can be accessed quickly. Finding a meaningful image from an archive is challenging research for the computer vision community (Latif et al., 2019).

Most search engines use traditional text-based algorithms that rely on captions and metadata to retrieve images. This technique can obtain images that are not relevant as there is a difference between human visual perception and manual categorization or tagging. IR based on image contents has become increasingly popular in recent decades and is regarded as one of the most effective methods of visual data access.

Content-based image retrieval (CBIR) is the visual content analysis of an image. The fundamental need for this IR method is to supply a query image as an input. The visual likeness in terms of image feature vector gives a basis for finding images with matching contents. Low-level visual features (like spatial layout, color, shape, and texture) are derived from the query in IR, and then these features are matched to rank the output.

Medical IR like skin cancer detection, microscopic pathology IR (Müller, 2020), trademark IR (Cao et al., 2021), fabric retrieval (Ji et al., 2020), and crime scene investigation using face retrieval (Tarawneh et al., 2018), tattoo retrieval (Lee et al., 2012), image searching in personal and public digital libraries and satellite IR, image analysis in traffic control (Tunio et al., 2020), image steganography (Shifa et al., 2018), and medical image diagnosis (Kayhan & Fekri-Ershad, 2021) are some of the applications of IR (Yang et al., 2021).

The effectiveness of feature extraction and description approaches determines the success of the IR method. The retrieved features convey the images' identities and aid retrieval. As a result, the researchers' attention has been drawn to the investigation for effective feature extraction and description approaches to investigate a higher success rate of IR based on image contents.

Image thresholding is an image segmentation method that uses pixel intensities to binarize the image pixels into the foreground or background. If the pixel's intensity exceeds the threshold, it is considered the foreground pixel; otherwise, it is considered a background pixel. The image thresholding techniques can be categorized as global or local. The global thresholding techniques use the same threshold for the whole image. In contrast, local thresholding techniques use different thresholds to separate the pixels into foreground or background in different parts of the image depending upon the local image regions. Here, feature fusion-based image retrieval is proposed using Sauvola local thresholding and SBTC techniques. The similarity is measured with the mean squared error (MSE) distance metric, and average retrieval accuracy is used as the performance metric. The key contributions of the work presented are as follows:

- Fusion of global and local features for improved image retrieval
- Consideration of Thepade's SBTC for extracting global features and Sauvola thresholding for local feature extraction.
- Exploration of weighted feature fusion of local and global features for image retrieval.
- Experimental validation of the proposed method on two benchmarked image datasets.

RELATED WORK

The image feature vector can be represented using global, local, and low-level features like texture, color, and shape. The feature vector based on color uses pixel intensities to represent the image. In comparison to other features, color features are consistent and robust. Most color attributes are unaffected by scale, translation, or rotation changes. The computational cost of simple color moment-based approaches is minimal, but the precision is low. Techniques based on histograms are more accurate, although they have a higher processing cost. Techniques based on BTC are more accurate and have a lower processing cost. "Color Coherence vector" (Pass et al., 1996), "Color Correlogram" (Huang et al., 1997), Block Truncation Coding(BTC) and its variants like "Optimized Dot Diffusion" (Guo & Liu, 2014), "error diffused BTC"(Guo et al., 2015), "halftoning based BTC" (Guo & Prasetyo, 2015), "Dot Diffused BTC (DDBTC)" (Guo et al., 2015), "ant colony optimization based BTC" (Chen et al., 2018), "Thepade's Sorted BTC(SBTC)," color moment-based techniques (Wang et al., 2018), histogram of colors-based techniques like "MPEG-7 Dominant Color Descriptor" (Shao et al., 2008) and "Fuzzy Histogram" (Han & Ma, 2002) are some of the color feature-based techniques.

Another important element in IR strategies is texture. An image's texture denotes the shift in illumination in a small area. An image's texture reflects the visual pattern by describing the spatial relationship of pixels. Statistical methods and structural approaches are the two types of texture-based algorithms. "Gray level histogram," "edge histogram," "local binary pattern(LBP)" (Ojala et al., 1996) and its variants like "Local Binary Extrema Pattern" (LBEP) (Murala et al., 2012b), "Local Tetra Pattern" (LTrP) (Murala et al., 2012a), "Local Derivative Pattern" (Zhang et al., 2010), "Utilizing multiscale LBP" (Srivastava & Khare, 2018), "gray level co-occurrence matrix(GLCM)"(Haralick et al., 1973), "wavelet coefficients" (Loupias et al., 2000), "ridgelets and curvelets" (Sumana et al., 2008), "Tamura features" (Tamura et al., 1978), and "Gabor wavelet filter" (Manjunath & Ma, 1996) are examples of texture-based feature techniques. Texture approaches based on structure are not effective for retrieving generic images. Statistical texture features are better than the other approaches because they are invariant to illumination, but the feature vector is larger.

In addition to texture and color features, shape features are explored in the literature to retrieve similar images since humans perceive objects based on their shape (Baji & Mocanu, 2018; Sun & Wu, 2006; Xiaoling & Kanglin, 2004). The use of shape-based features for IR is limited since these approaches require segmented object images, which are tough to obtain in datasets with non-homogeneous generic images.

Local features-based techniques locate prominent parts termed interest points and describe the image by expressing the surrounding region of these interest points. The detected interest points must be extremely repetitive to be identified with several distortions like rotation and light. Some of the most often used strategies for detecting local features are “Harris corner detector” (Harris & Stephens, 1988), “Fast Hessian” (Bay et al., 2006), “Hessian affine detector” (Mikolajczyk & Schmid, 2002), “Harris-Laplace” (Mikolajczyk & Schmid, 2001), “Shi and Tomasi corner detector” (Shi & Tomasi, 1994), “Difference of Gaussian” (Lowe, 2004), MSER, (Matas et al., 2004) SUSAN (Smith & Brady, 1997), FAST (Rosten & Drummond, 2006), SIFT and its variants like “PCA-SIFT” (Ke & Sukthankar, 2004), “N-SIFT” (Cheung & Hamarneh, 2007), “CSIFT” (Abdel-Hakim & Farag, 2006), “edge-SIFT” (Zhang et al., 2013), “Color-SIFT” (Van De Sande et al., 2010), “Affine-SIFT”(Yu & Morel, 2011), “root-SIFT” (Arandjelovic & Zisserman, 2012), BRISK (Leutenegger et al., 2011), ORB (Rublee et al., 2011), BRIEF (Calonder et al., 2010), SURF (Bay et al., 2006) and FREAK (Alahi et al., 2012). These techniques generate high-dimensional feature vectors and thus require more memory for storage and matching time during query execution.

Jabeen et al. (2018) combine a bag of visual words (BoVW) with FREAK and SURF local feature extraction algorithms. Dhotre and Bamnote (2017) integrate multilevel Haar wavelet features with a color histogram. Color and edge features are integrated into Hua et al. (2019) to create a resilient color volume histogram-based feature vector. The BoVW technique is paired with SURF and SIFT-based features in Alkhawlani et al. (2015). The features of chromaticity moments, co-occurrence, and color moments are combined to form a feature vector in Singh and Srivastava (2018). Local and global properties are fused in Mehmood et al. (2018) by considering the image’s Histogram of Gradient (HoG) and SURF features. In Alhassan and Alfaki (2017), HSV color moments and texture features based on the 2D Gabor filter are presented. In Mistry et al. (2016), the feature descriptor is generated using a fusion of DWT in YCbCr color space and LBP. In Du et al. (2019), a weighted fusion of HSV color space-based histogram, GLCM, LBP, and normalized moment of inertia (NMI) with particle swarm optimization-based pulse code neural network (PCNN) is proposed. Yu et al. (2013) present the fusion of SIFT and LBP features with the Kmeans clustering algorithm.

Also, in the literature, few IR methods use the weighted fusion of color and texture features (Kayhan & Fekri-Ershad, 2021). Few authors have proposed using quantized color bins with tetrolet transform for image retrieval (Varish et al., 2020).

Image datasets have images that are widely diversified and non-homogeneous. Using simple and individual low-level image features to retrieve the matching images is quite challenging. As a result, in the literature, integrating low-level features (color, shape, and texture), global features, and local features for encoding feature vectors has improved the performance of IR algorithms.

Here, the weighted feature fusion of the color-based Sauvola local thresholding technique with global SBTC to generate the feature vector of the image is presented.

THEPADE'S SORTED BLOCK TRUNCATION CODING (SBTC)

Let the image block be 'B' of size 'a x b x 3', with R, G, and B color planes. The SBTC n-ary can be represented as [FR₁, FR₂, ..., FR_n, FG₁, FG₂, ..., FG_n, FB₁, FB₂, ..., FB_n]. Here the FR_p, FG_p, and FB_p indicate the pth cluster centroids of the red, green, and blue planes, respectively (Dewan & Thepade, 2021).

The feature extraction using SBTC is shown in Figure 1. Here, for the sample input image, the color planes are extracted, which are further converted to a 1D array for getting sorted. In the end, features are generated by clustering these sorted 1D arrays. In SBTC 4-ary, for image block B of size 'a x b x 3' pixels, the color planes R, G, and B are converted into a one-dimensional array and sorted as sR, sG, and sB. The sorted 1D arrays are divided into four equal-size clusters. The centroid of each cluster is computed as [FR₁, FR₂, FR₃, FR₄, FG₁, FG₂, FG₃, FG₄, FB₁, FB₂] as shown in Equations 1 to 4. Here, X= R, G, or B.

$$FX_1 = \frac{4}{a * b} \sum_{r=1}^{\frac{a*b}{4}} sX(r) \quad (1)$$

$$FX_2 = \frac{4}{a * b} \sum_{r=1+\frac{a*b}{4}}^{\frac{a*b}{2}} sX(r) \quad (2)$$

$$FX_3 = \frac{4}{a * b} \sum_{r=1+\frac{a*b}{2}}^{\frac{3*a*b}{4}} sX(r) \quad (3)$$

$$FX_4 = \frac{4}{a * b} \sum_{r=1+\frac{3*a*b}{4}}^{a*b} sX(r) \quad (4)$$

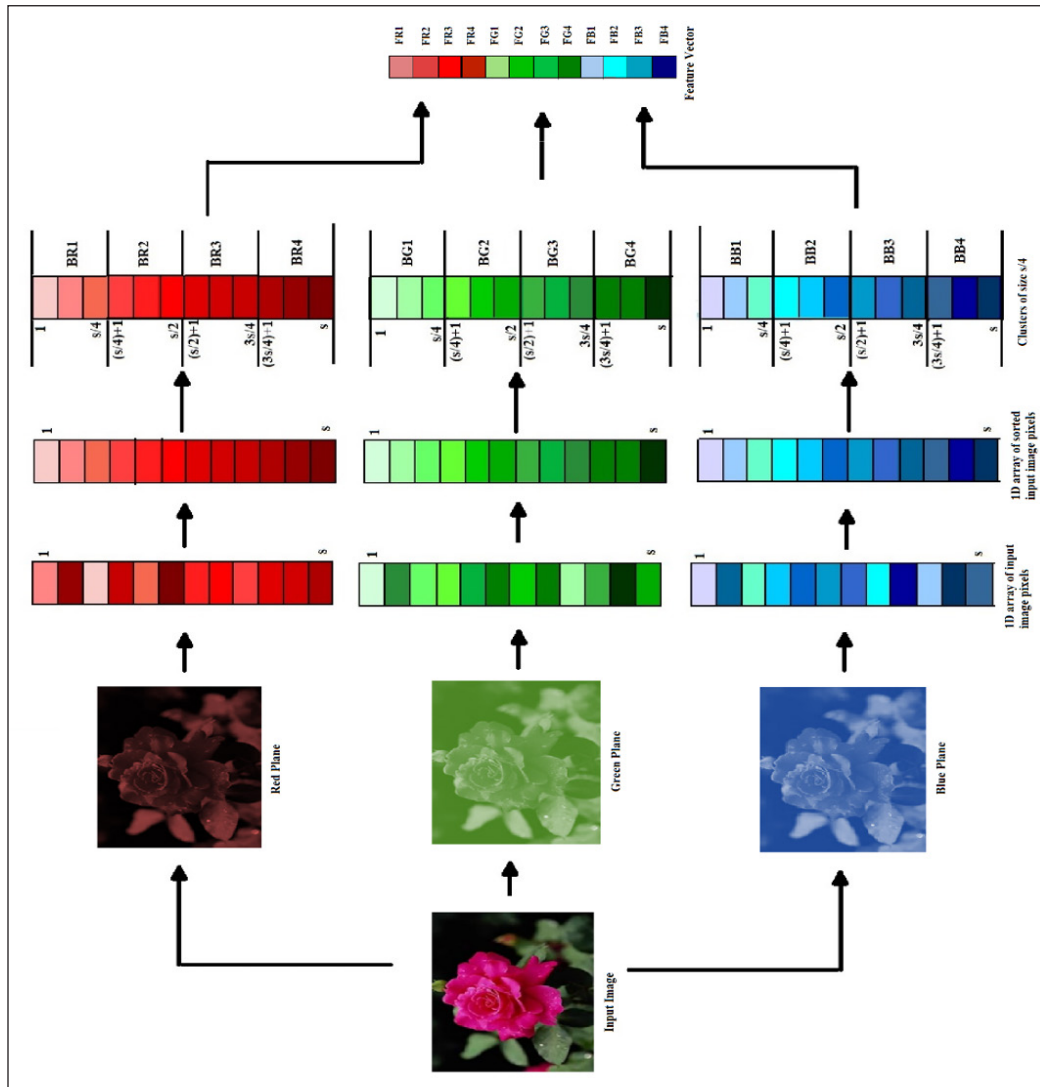


Figure 1. Feature vector generation using SBTC

SAUVOLA THRESHOLDING TECHNIQUE

It is a local thresholding method that determines the threshold for each pixel. The threshold is calculated using a local variance. The technique is effective when the image's brightness is not constant (Bataineh et al., 2011; Hadjadj et al., 2016; Lazzara & Géraud, 2014; Sauvola & Pietikäinen, 2000).

The threshold for each pixel is calculated using Equations 5, 6, and 7:

$$T_{(p,q)} = \text{Mean}_{(p,q)} * \left[1 + k * \left(\frac{\text{dev}_{(p,q)}}{D} - 1 \right) \right] \quad (5)$$

$$dev_{(p,q)} = \sqrt{\frac{1}{x * y} \sum_{x=1}^3 \sum_{y=1}^3 I(x,y)^2 - \left[\frac{1}{x * y} \sum_{x=1}^3 \sum_{y=1}^3 I(x,y) \right]^2} \quad (6)$$

$$D = \max(dev) \quad (7)$$

where,

$T(p,q)$ is the threshold for the pixel position in the image at (p,q) , where p is the row number, and q is the column number of the pixel.

$\text{Mean}(p,q)$ and $\text{dev}(p,q)$ are the average and standard deviation using the intensity values of the pixels present in the window centered at the (p,q) pixel in the image.

$I(x,y)$ represents the intensity of the neighborhood pixel located at the (x,y) position in the image.

k is the user-defined constant, and D is the dynamic range of standard deviation.

Figure 2 portrays the extraction of binary planes from red, green, and blue color components of the original sample image obtained using the Sauvola thresholding technique. As the Sauvola threshold values for respective color planes differ, the binary color planes also differ.

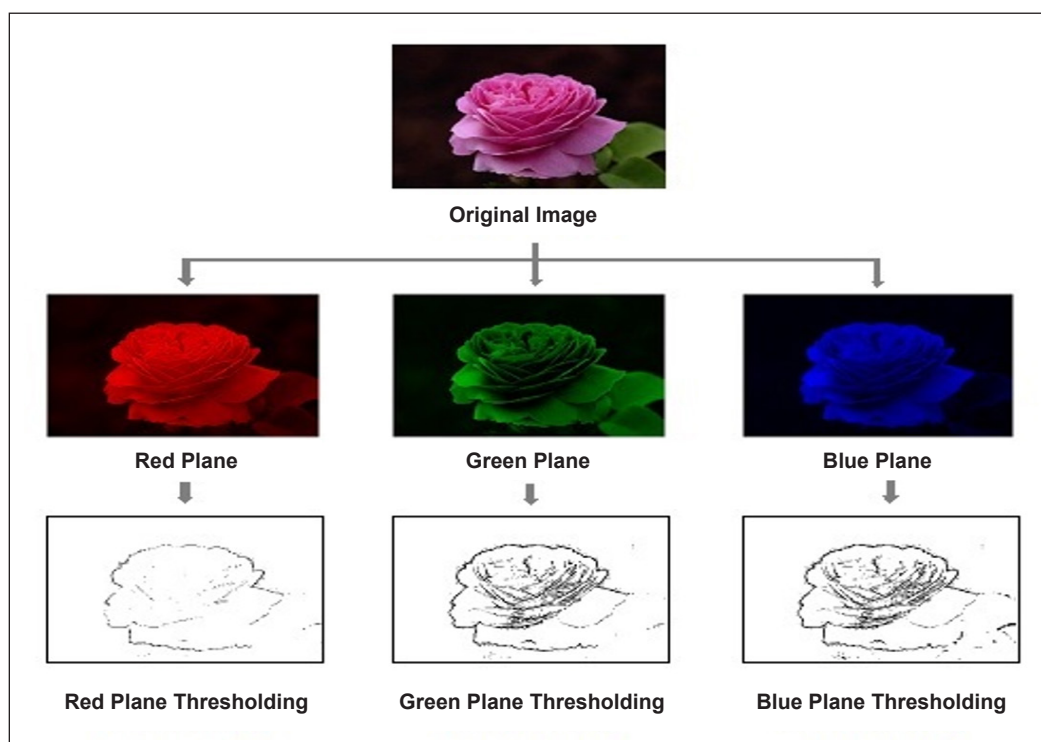


Figure 2. Sauvola local thresholding

PROPOSED IMAGE RETRIEVAL TECHNIQUE

The block diagram of the proposed weighted fusion-based IR system using SBTC and Sauvola Local Thresholding (SLT) features is shown in Figure 3. The steps for image feature vector detection and description are given in the algorithm.

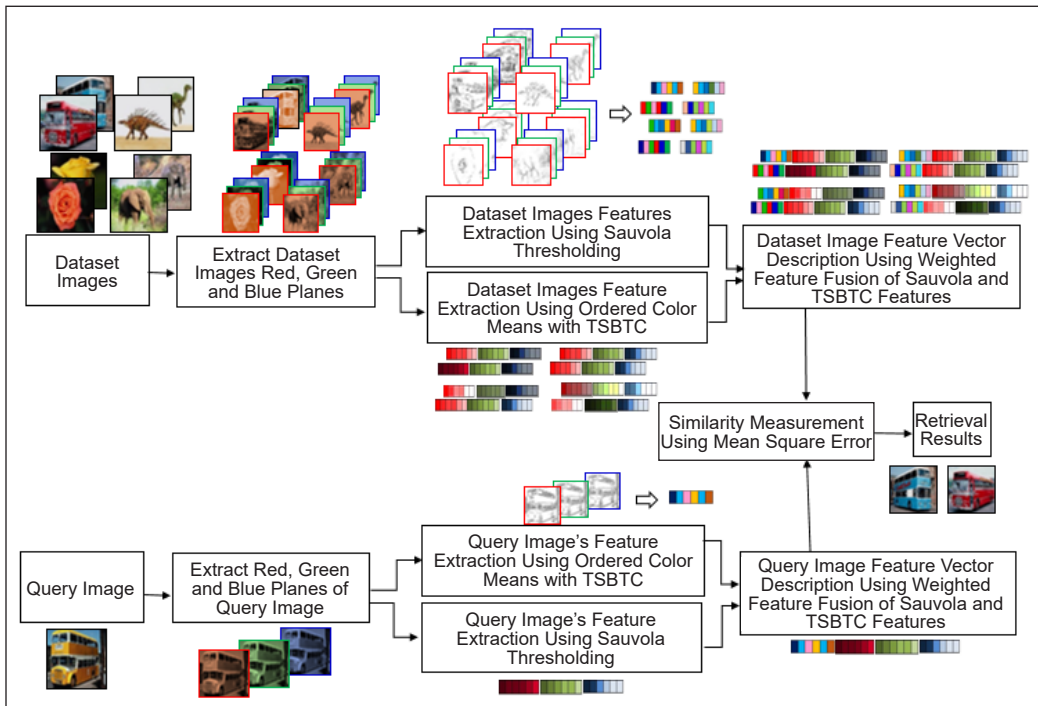


Figure 3. Block diagram of weighted feature fusion-Based IR using Sauvola and SBTC features

Algorithm

1. Input the image color image I of size $mxnx3$ with red R_i , green G_i , and blue B_i planes.
2. Generate the SBTC color feature vector by applying steps 2.1 to 2.5.
 - 2.1 Convert the color plane of size mxn into $(mn) \times 1$ size one-dimensional array (SDA).
 - 2.2 Sort the pixel intensity values of the SDA array in ascending order.
 - 2.3 Divide the array SDA into N blocks where N is 2-ary, 4-ary, or 8-ary of SBTC selected.
 - 2.4 Find the mean of pixel values for each block. These mean values form the color feature vector of an image plane.
 - 2.5 Apply steps 2.1 to 2.4 on an image's red, green, and blue planes. An image's color-based feature vector F_c is formed by concatenating the features of all the planes.

3. Generate Sauvola thresholding-based feature vector by applying steps 3.1 to 3.5 (Figure 2).
 - 3.1 The color image is separated into red, green, and blue planes.
 - 3.2 Compute the threshold T_x for each image pixel red, green, and blue plane using Equations 5, 6, and 7.
 - 3.3 Compute the bitmap of all the color planes of the image using Equation 8. Let I_j be the j th color plane of image I , T_j be the threshold of color plane I_j , and B_j be the binary plane of the I_j color plane. The pixel positions are represented as (p,q) .

$$B_j(p, q) = \begin{cases} 1, & \text{if } I_j(p, q) \geq T_j(p, q) \\ 0, & \text{if } I_j(p, q) < T_j(p, q) \end{cases} \quad (8)$$

- 3.4 Generate Sauvola features S_{j1} and S_{j2} of the given image for each color plane with size $m*n$ using Equations 9 and 10. Here (a,b) indicates the pixel position.

$$S_{j1} = \frac{1}{\sum_{a=1}^m \sum_{b=1}^n B_j(a, b)} \left\{ \sum_{a=1}^m \sum_{b=1}^n [I_j(a, b) * B_j(a, b)] \right\} \quad (9)$$

$$S_{j2} = \frac{1}{\sum_{a=1}^m \sum_{b=1}^n (1 - B_j(a, b))} \left\{ \sum_{a=1}^m \sum_{b=1}^n [I_j(a, b) * (1 - B_j(a, b))] \right\} \quad (10)$$

- 3.5 Concatenate the Sauvola features F_s of all the color planes to generate the vector of the Sauvola local thresholding image features.
4. The fusion-based feature vector F_v is generated by concatenating the SBTC color-based feature vector F_c multiplied by weight $w1$ and Sauvola thresholding-based feature vector F_s multiplied by weight $w2$.
5. Steps 1 to 4 are applied to all the images of the dataset.
6. During query execution, steps 1–4 are applied to the query image.
7. The query image's feature vector is compared to the dataset image's feature vectors using mean square error (MSE) as the distance measure. Images with the shortest distance are deemed more relevant and are retrieved from the dataset.

In the case of the Sauvola thresholding technique, the mean of image pixel intensities greater than the threshold and the mean of image pixel intensities less than the threshold are used to represent the feature vector for each image. It has generated a feature size of two for each image plane. SBTC 8-ary has generated the feature of size eight for each image plane. The feature vector size is independent of the image dimension and has a considerably smaller footprint. The similarity is measured with

the mean squared error (MSE) distance metric, and average retrieval accuracy is used as the performance metric.

Image Dataset Used for Experimentation

Various datasets are published in the literature. Images of artificial things like monuments, landscapes, creatures, and natural sceneries such as beaches, mountains, and water can be found in these datasets. The images were captured under various lighting, rotation, scale, and occlusion settings. The experimentation testbed is built using a modified COIL dataset and an augmented version of the standard image dataset generated by Wang.

There are 1100 images in the augmented Wang (AWang) dataset, divided into 11 categories. Figure 4 depicts sample images of the AWang dataset (J. Z. Wang et al., 2001; Li & Wang, 2003).

The modified COIL(MCOIL) dataset contains 1440 photos. The images depict a variety of products from several categories, such as toys, pharmaceutical boxes, and coffee mugs. The objects were placed on a turntable with a dark background to capture these images in PNG format. Figure 5 displays a sample of images from the MCOIL dataset (Nene et al., n.d.).

			
Tribes	Beach	Monuments	Fooditems
			
Buses	Dinasour	Elephant	Aeroplane
			
Roses	Horses	Mountains	

Figure 4. AWang dataset sample images

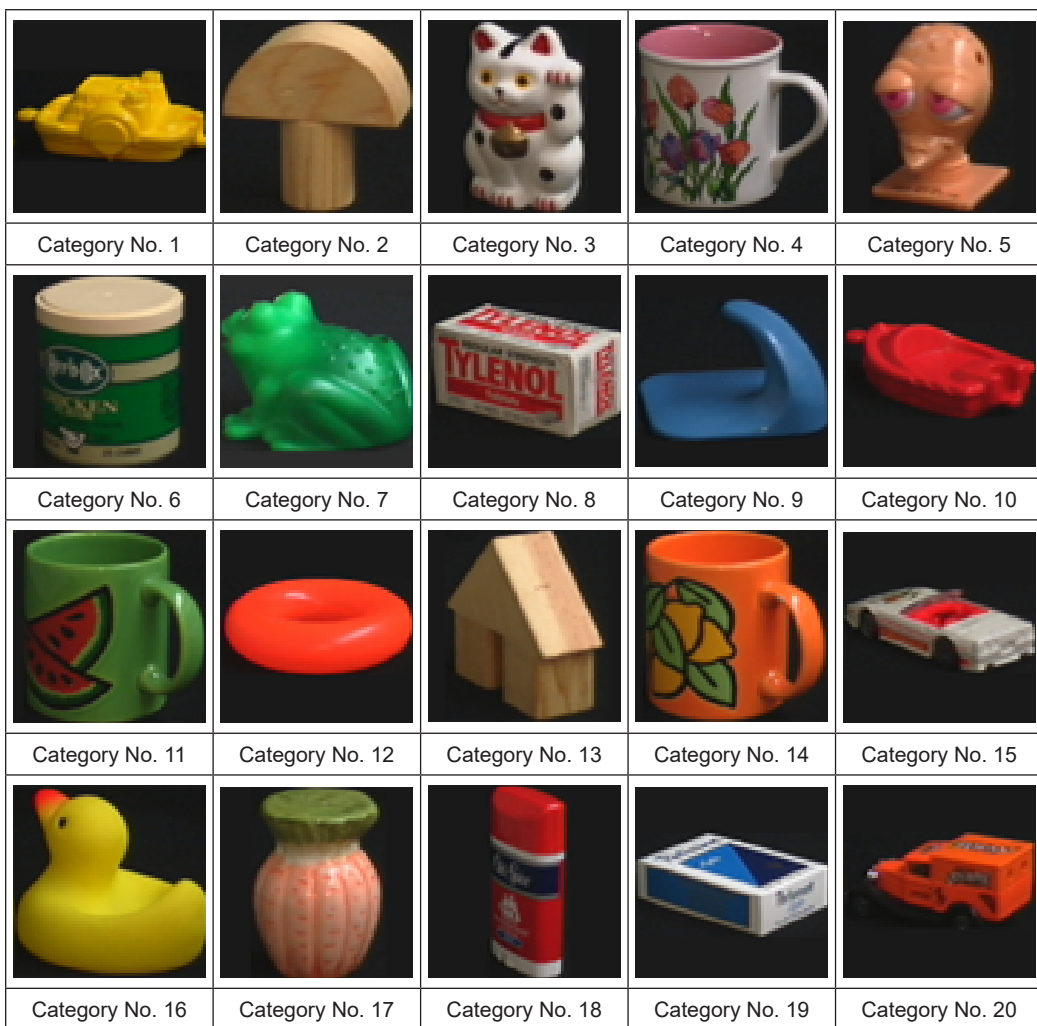


Figure 5. MCOIL dataset sample images

Performance Measurement Criteria

The retrieval accuracy is used to assess the quality of the IR system. Query images are fired on the image dataset. The query image feature vector is extracted and matched to the dataset image feature vectors, and the mean square error (MSE) is computed. The computed MSEs are sorted in ascending order to rank the dataset images to the query image. Relevant and irrelevant images are separated from the obtained images. The average retrieval accuracy is used for the performance measuring criterion. The definition of retrieval accuracy is given in Equation 11.

$$\text{Retrieval accuracy} = \frac{\text{significant images retrieved count}}{\text{total images retrieved count}} \quad (11)$$

The presented IR system is tested using MATLAB on an Intel Core i5 Processor computer with 1.7 GHz processing speed and 8 GB RAM.

RESULTS AND DISCUSSION

AWang and MCOIL datasets are used in the experimentation. The image feature vectors are generated from extracted features of the dataset images. In a feature table, these feature vectors are stored. During query execution, features from the query image are extracted, and a feature vector is created. This feature vector is compared to the dataset image feature vectors using MSE to extract matched photos from the dataset.

Tables 1 and 2 indicate the ARA of Sauvola Local Thresholding (SLT) and SBTC feature fusion techniques for AWang and MCOIL datasets with equal proportions, respectively. Results prove that the SLT and SBTC feature fusion-based technique results better ARA than the individual methods.

Table 1
IR using feature fusion of SLT and SBTC features for AWang dataset

Category	SLT	SBTC 2-ary	SLT + SBTC 2-ary	SBTC 4-ary	SLT + SBTC 4-ary	SBTC 8-ary	SLT + SBTC 8-ary
C1	39.56	30.65	35.58	32.51	35.27	33.36	34.78
C2	18.02	22.56	22.41	24.01	23.9	24.66	24.64
C3	20.63	18.74	20.5	18.69	19.56	18.97	19.43
C4	34.25	33.03	37.09	33.03	35.85	32.58	34.12
C5	97.4	95.68	96.29	95.58	96.07	95.28	95.66
C6	32.08	37.31	37.64	37.08	37.42	37.13	37.25
C7	54.13	43.11	48.2	41.89	44.97	42.77	44.38
C8	40.58	49.77	48.2	50.74	50	50.48	50.29
C9	18.6	22.7	21.14	21.82	21.04	21.67	21.38
C10	27.96	27.27	28.41	27.39	28.38	28	28.42
C11	67.04	71.26	72.45	74.07	74.55	74.12	74.68
ARA (%)	40.93	41.10	42.54	41.53	42.46	41.73	42.28

Table 2
IR using feature fusion of SLT and SBTC features for MCOIL dataset

Category	SLT	SBTC 2-ary	SLT + SBTC 2-ary	SBTC 4-ary	SLT + SBTC 4-ary	SBTC 8-ary	SLT + SBTC 8-ary
1	45.62	42.38	43.42	47.01	47.16	46.97	47.05
2	55.67	43.07	51.52	40.63	43.69	37.06	38.29
3	60.57	61.84	64.00	75.52	78.01	77.78	79.53
4	68.44	72.55	75.77	93.71	94.58	96.89	97.03
5	89.33	98.90	98.80	99.61	99.48	99.81	99.92
6	100.00	98.59	100.00	99.98	100.00	100.00	100.00

Table 2 (*continue*)

Category	SLT	SBTC 2-ary	SLT + SBTC 2-ary	SBTC 4-ary	SLT + SBTC 4-ary	SBTC 8-ary	SLT + SBTC 8-ary
7	83.06	80.73	84.66	82.74	85.07	83.16	84.49
8	55.11	47.55	53.13	54.07	56.33	54.46	55.59
9	97.55	99.92	99.71	100.00	100.00	100.00	100.00
10	51.25	42.26	46.20	47.80	48.92	48.11	48.96
11	100.00	100.00	100.00	100.00	100.00	100.00	100.00
12	98.92	100.00	100.00	100.00	100.00	100.00	100.00
13	39.85	34.39	38.37	31.58	33.89	30.48	31.50
14	93.36	85.90	90.78	89.22	90.68	89.85	90.59
15	51.52	45.54	48.73	47.70	49.59	46.53	47.92
16	78.07	82.21	80.50	79.57	79.34	79.05	78.92
17	95.60	96.49	99.42	100.00	100.00	100.00	100.00
18	57.16	43.25	50.14	48.90	51.76	50.91	52.47
19	69.68	61.79	64.47	62.73	63.70	61.92	62.58
20	54.24	46.59	50.83	50.81	52.28	51.99	52.64
ARA (%)	72.25	69.20	72.02	72.58	73.72	72.75	73.37

Table 3 indicates the ARA for weighted SLT and SBTC 2-ary feature fusion using the AWang dataset. The fusion of 0.7 for SLT and 0.3 for SBTC 2-ary features performs better than other proportions considered.

Table 3
IR using weighted SLT and SBTC 2-ary feature fusion for AWang dataset

Category	SLT	SBTC 2-ary		SLT: 0.9 SBTC: 0.1	SLT: 0.8 SBTC: 0.2	SLT: 0.7 SBTC: 0.3	SLT: 0.6 SBTC: 0.4	SLT: 0.5 SBTC: 0.5	SLT: 0.4 SBTC: 0.6	SLT: 0.3 SBTC: 0.7	SLT: 0.2 SBTC: 0.8	SLT: 0.1 SBTC: 0.9	
C1	39.56	30.65	39.14	38.44	37.68	36.6	35.58	34.55	33.6	32.7	31.68		
C2	18.02	22.56	19.77	20.9	21.74	22.06	22.41	22.77	22.83	22.84	22.82		
C3	20.63	18.74	20.99	21.2	21.18	20.81	20.5	20.14	19.77	19.51	19.05		
C4	34.25	33.03	36.57	37.7	37.88	37.76	37.09	36.58	35.74	34.79	33.9		
C5	97.4	95.68	97.33	96.91	96.64	96.42	96.29	96.12	95.97	95.91	95.75		
C6	32.08	37.31	34.01	35.65	36.73	37.31	37.64	37.81	37.67	37.59	37.46		
C7	54.13	43.11	52.93	51.66	50.27	49.33	48.2	47.18	46.01	44.89	43.91		
C8	40.58	49.77	43.23	45.13	46.52	47.49	48.2	48.72	49.14	49.3	49.59		
C9	18.6	22.7	19.3	19.94	20.29	20.79	21.14	21.43	21.96	22.19	22.52		
C10	27.96	27.27	28.38	28.72	28.66	28.54	28.41	28.22	28	27.81	27.52		
C11	67.04	71.26	69.47	70.85	71.65	72.16	72.45	72.39	72.27	71.94	71.56		
ARA(%)	40.93	41.10	41.92	42.46	42.66	42.54	42.36	42.09	41.77	41.43			

Table 4 indicates the ARA for weighted SLT and SBTC 4-ary feature fusion using the AWang dataset. The fusion of 0.8 for SLT and 0.2 for SBTC 4-ary features performs better than other proportions considered.

Table 4
IR using weighted SLT and SBTC 4-ary feature fusion for AWang dataset

Category	SLT	SBTC 4-ary	SLT: 0.9 SBTC: 0.1	SLT: 0.8 SBTC: 0.2	SLT: 0.7 SBTC: 0.3	SLT: 0.6 SBTC: 0.4	SLT: 0.5 SBTC: 0.5	SLT: 0.4 SBTC: 0.6	SLT: 0.3 SBTC: 0.7	SLT: 0.2 SBTC: 0.8	SLT: 0.1 SBTC: 0.9
C1	39.56	32.51	39.15	37.92	36.94	36.11	35.27	34.59	33.84	33.18	32.87
C2	18.02	24.01	21.48	22.93	23.51	23.71	23.9	24.05	24.06	24.01	24.00
C3	20.63	18.69	20.86	20.7	20.36	20	19.56	19.39	19.06	18.92	18.77
C4	34.25	33.03	37.99	38.05	37.37	36.49	35.85	35.1	34.45	33.96	33.47
C5	97.4	95.58	96.86	96.45	96.29	96.21	96.07	95.94	95.87	95.78	95.68
C6	32.08	37.08	35.5	36.78	37.27	37.44	37.42	37.4	37.33	37.29	37.23
C7	54.13	41.89	51.17	49.17	47.36	45.94	44.97	44.12	43.45	42.87	42.35
C8	40.58	50.74	45.39	47.86	48.87	49.54	50	50.26	50.37	50.45	50.64
C9	18.6	21.82	19.8	20.1	20.49	20.83	21.04	21.34	21.36	21.45	21.68
C10	27.96	27.39	28.92	28.88	28.8	28.59	28.38	28.21	28.03	27.79	27.61
C11	67.04	74.07	71.73	73.5	74.14	74.62	74.55	74.48	74.35	74.25	74.19
ARA (%)	40.93	41.53	42.62	42.94	42.85	42.68	42.46	42.26	42.02	41.81	41.68

Table 5 indicates the ARA for weighted SLT and SBTC 8-ary feature fusion using the AWang dataset. The fusion of 0.9 for SLT and 0.1 for SBTC 8-ary features performs better than other proportions considered.

Table 5
IR using weighted SLT and SBTC 8-ary feature fusion for AWang dataset

Category	SLT	SBTC 8-ary	SLT: 0.9 SBTC: 0.1	SLT: 0.8 SBTC: 0.2	SLT: 0.7 SBTC: 0.3	SLT: 0.6 SBTC: 0.4	SLT: 0.5 SBTC: 0.5	SLT: 0.4 SBTC: 0.6	SLT: 0.3 SBTC: 0.7	SLT: 0.2 SBTC: 0.8	SLT: 0.1 SBTC: 0.9
C1	39.56	33.36	38.32	37.02	36.08	35.35	34.78	34.33	34.03	33.72	33.53
C2	18.02	24.66	23.11	23.93	24.46	24.6	24.64	24.68	24.69	24.72	24.74
C3	20.63	18.97	20.8	20.24	19.87	19.64	19.43	19.24	19.12	19.04	18.98
C4	34.25	32.58	37.89	36.64	35.49	34.74	34.12	33.6	33.27	32.99	32.76
C5	97.4	95.28	96.41	96.2	95.97	95.76	95.66	95.52	95.43	95.37	95.33
C6	32.08	37.13	36.87	37.31	37.52	37.41	37.25	37.25	37.24	37.25	37.19
C7	54.13	42.77	49.75	47.22	45.81	45.01	44.38	43.91	43.52	43.19	42.93
C8	40.58	50.48	47.68	49.19	49.76	50.07	50.29	50.46	50.44	50.46	

Table 5 (*continue*)

Category	SLT	SBTC 8-ary	SLT: 0.9 SBTC: 0.1	SLT: 0.8 SBTC: 0.2	SLT: 0.7 SBTC: 0.3	SLT: 0.6 SBTC: 0.4	SLT: 0.5 SBTC: 0.5	SLT: 0.4 SBTC: 0.6	SLT: 0.3 SBTC: 0.7	SLT: 0.2 SBTC: 0.8	SLT: 0.1 SBTC: 0.9
C9	18.6	21.67	20.11	20.49	20.95	21.3	21.38	21.41	21.59	21.68	21.7
C10	27.96	28	29.18	29.09	28.8	28.65	28.42	28.27	28.22	28.18	28.1
C11	67.04	74.12	73.86	74.77	74.97	74.79	74.68	74.47	74.34	74.3	74.18
ARA (%)	40.93	41.73	43.09	42.92	42.70	42.48	42.28	42.10	41.99	41.90	41.81

Table 6 indicates the ARA for weighted SLT and SBTC 2-ary feature fusion using the MCOIL dataset. The fusion of 0.8 for SLT and 0.2 for SBTC 2-ary features performs better than other proportions considered.

Table 6
IR using weighted SLT and SBTC 2-ary feature fusion for MCOIL dataset

Category	SLT	SBTC 2-ary	SLT: 0.9 SBTC: 0.1	SLT: 0.8 SBTC: 0.2	SLT: 0.7 SBTC: 0.3	SLT: 0.6 SBTC: 0.4	SLT: 0.5 SBTC: 0.5	SLT: 0.4 SBTC: 0.6	SLT: 0.3 SBTC: 0.7	SLT: 0.2 SBTC: 0.8	SLT: 0.1 SBTC: 0.9
1	45.62	42.38	44.83	44.06	43.89	43.63	43.42	43.17	42.94	42.61	42.46
2	55.67	43.07	54.36	53.67	52.95	52.28	51.52	50.46	49.23	47.45	45.47
3	60.57	61.84	62.94	64.14	64.45	64.43	64.00	63.54	63.14	62.71	62.29
4	68.44	72.55	72.86	75.04	76.08	76.18	75.77	75.29	74.50	73.65	73.07
5	89.33	98.90	93.06	95.58	97.24	98.28	98.80	99.09	99.29	99.34	99.25
6	100.0	98.59	100.0	100.0	100.0	100.0	100.0	100.0	100.0	100.0	99.86
7	83.06	80.73	84.59	85.44	85.88	85.59	84.66	83.74	83.14	82.52	81.50
8	55.11	47.55	55.21	54.84	54.48	53.94	53.13	52.24	51.20	49.98	48.50
9	97.55	99.92	98.44	99.02	99.31	99.56	99.71	99.83	99.88	99.88	99.92
10	51.25	42.26	49.98	49.21	48.42	47.30	46.20	45.02	43.98	43.19	42.80
11	100.0	100.0	100.0	100.0	100.0	100.0	100.0	100.0	100.0	100.0	100.0
12	98.92	100.0	99.56	99.90	100.0	100.0	100.0	100.0	100.0	100.0	100.0
13	39.85	34.39	39.12	38.54	38.14	38.00	38.37	38.10	37.60	36.52	35.19
14	93.36	85.90	93.54	93.04	92.42	91.51	90.78	89.99	88.99	88.02	87.02
15	51.52	45.54	50.52	49.90	49.40	49.02	48.73	48.32	47.74	46.99	46.24
16	78.07	82.21	78.82	79.44	79.90	80.09	80.50	80.81	81.17	81.58	81.93
17	95.60	96.49	97.03	98.01	98.59	99.00	99.42	99.59	99.77	99.85	99.75
18	57.16	43.25	55.96	55.02	53.65	51.99	50.14	48.44	46.91	45.58	44.21
19	69.68	61.79	68.00	66.99	65.99	65.03	64.47	63.83	63.18	62.79	62.38
20	54.24	46.59	53.38	52.68	51.99	51.49	50.83	50.12	49.36	48.53	47.70
ARA (%)	72.25	69.20	72.61	72.73	72.64	72.36	72.02	71.58	71.10	70.56	69.98

Table 7 indicates the ARA for weighted SLT and SBTC 4-ary feature fusion using the MCOIL dataset. The fusion of 0.9 for SLT and 0.1 for SBTC 4-ary features performs better than other proportions considered.

Table 8 indicates the ARA for weighted SLT and SBTC 8-ary feature fusion using the MCOIL dataset. The fusion of 0.9 for SLT and 0.1 for SBTC 8-ary features performs better than other proportions considered.

Comparison with Existing Methods

Figures 6 and 7 show the performance of existing and proposed IR techniques in terms of ARA using Sauvola local thresholding, SBTC with 2, 4, and 8-arys, and weighted feature fusion of SLT and SBTC for AWang and MCOIL datasets, respectively. Weighted feature fusion of SLT and SBTC performs better for SBTC 2, 4, and 8-arys. Results show that the fusion of 0.9 for SLT and 0.1 for SBTC 8-ary features gives better results than all other methods considered.

Table 7
IR using weighted SLT and SBTC 4-ary feature fusion for MCOIL dataset

Category	SLT	SBTC 4-ary	SLT: 0.9 SBTC: 0.1	SLT: 0.8 SBTC: 0.2	SLT: 0.7 SBTC: 0.3	SLT: 0.6 SBTC: 0.4	SLT: 0.5 SBTC: 0.5	SLT: 0.4 SBTC: 0.6	SLT: 0.3 SBTC: 0.7	SLT: 0.2 SBTC: 0.8	SLT: 0.1 SBTC: 0.9
1	45.62	47.01	47.11	47.30	47.26	47.26	47.16	47.07	47.05	47.01	46.99
2	55.67	40.63	51.60	48.63	46.64	44.75	43.69	42.75	42.01	41.42	40.93
3	60.57	75.52	77.16	79.17	79.07	78.40	78.01	77.53	76.93	76.41	75.98
4	68.44	93.71	93.61	95.06	95.10	94.85	94.58	94.43	94.17	94.04	93.81
5	89.33	99.61	95.56	98.09	99.00	99.36	99.48	99.59	99.61	99.59	99.61
6	100.0	99.98	100.0	100.0	100.0	100.0	100.0	100.0	100.0	100.0	100.0
7	83.06	82.74	87.83	87.87	86.81	85.82	85.07	84.43	84.09	83.58	83.08
8	55.11	54.07	57.37	57.75	57.25	56.75	56.33	55.90	55.40	54.96	54.53
9	97.55	100.0	99.38	99.96	100.0	100.0	100.0	100.0	100.0	100.0	100.0
10	51.25	47.80	51.08	50.39	50.02	49.54	48.92	48.51	48.28	48.19	47.99
11	100.0	100.0	100.0	100.0	100.0	100.0	100.0	100.0	100.0	100.0	100.0
12	98.92	100.0	100.0	100.0	100.0	100.0	100.0	100.0	100.0	100.0	100.0
13	39.85	31.58	37.09	36.28	35.19	34.61	33.89	33.41	32.89	32.41	31.96
14	93.36	89.22	93.77	92.82	91.96	91.24	90.68	90.28	90.01	89.66	89.39
15	51.52	47.70	51.49	50.93	50.42	49.88	49.59	49.21	48.80	48.40	47.97
16	78.07	79.57	78.72	78.99	79.11	79.24	79.34	79.42	79.51	79.53	79.53
17	95.60	100.00	99.50	99.88	99.98	100.0	100.0	100.0	100.0	100.0	100.0
18	57.16	48.90	56.54	55.48	54.01	52.78	51.76	50.96	50.42	49.85	49.29
19	69.68	62.73	67.11	65.66	64.62	64.08	63.70	63.41	63.21	62.96	62.83
20	54.24	50.81	53.55	52.82	52.78	52.51	52.28	51.93	51.58	51.33	51.04
ARA (%)	72.25	72.58	74.92	74.85	74.46	74.05	73.72	73.44	73.20	72.97	72.75

Table 8
IR using weighted SLT and SBTC 8-ary feature fusion for MCOIL dataset

Category	SLT	SBTC 8-ary	SLT: 0.9 SBTC: 0.1	SLT: 0.8 SBTC: 0.2	SLT: 0.7 SBTC: 0.3	SLT: 0.6 SBTC: 0.4	SLT: 0.5 SBTC: 0.5	SLT: 0.4 SBTC: 0.6	SLT: 0.3 SBTC: 0.7	SLT: 0.2 SBTC: 0.8	SLT: 0.1 SBTC: 0.9
1	45.62	46.97	47.38	47.18	47.18	47.09	47.05	47.03	47.01	47.01	46.97
2	55.67	37.06	45.29	41.67	39.87	38.91	38.29	37.83	37.64	37.42	37.23
3	60.57	77.78	81.33	80.92	80.50	79.92	79.53	79.13	78.53	78.24	78.03
4	68.44	96.89	96.66	97.18	97.13	97.11	97.03	96.93	96.82	96.88	96.88
5	89.33	99.81	98.77	99.71	99.85	99.88	99.92	99.92	99.86	99.86	99.85
6	100.00	100.00	100.00	100.00	100.00	100.00	100.00	100.00	100.00	100.00	100.00
7	83.06	83.16	88.10	86.65	85.53	84.80	84.49	84.09	83.89	83.66	83.37
8	55.11	54.46	58.45	57.52	56.64	55.90	55.59	55.23	54.94	54.76	54.57
9	97.55	100.00	100.00	100.00	100.00	100.00	100.00	100.00	100.00	100.00	100.00
10	51.25	48.11	51.23	50.35	49.75	49.36	48.96	48.71	48.55	48.32	48.19
11	100.00	100.00	100.00	100.00	100.00	100.00	100.00	100.00	100.00	100.00	100.00
12	98.92	100.00	100.00	100.00	100.00	100.00	100.00	100.00	100.00	100.00	100.00
13	39.85	30.48	35.24	33.28	32.27	31.87	31.50	31.33	31.00	30.92	30.65
14	93.36	89.85	93.09	91.90	91.24	90.76	90.59	90.41	90.18	90.03	89.97
15	51.52	46.53	50.42	49.46	48.84	48.30	47.92	47.51	47.18	46.91	46.70
16	78.07	79.05	78.61	78.72	78.88	78.84	78.92	78.95	78.95	78.99	79.01
17	95.60	100.00	100.00	100.00	100.00	100.00	100.00	100.00	100.00	100.00	100.00
18	57.16	50.91	57.06	54.76	53.65	53.09	52.47	52.01	51.54	51.23	51.06
19	69.68	61.92	65.14	63.91	63.16	62.83	62.58	62.42	62.31	62.17	62.06
20	54.24	51.99	53.88	53.36	53.16	52.91	52.64	52.53	52.33	52.16	52.08
ARA (%)	72.25	72.75	75.03	74.33	73.88	73.58	73.37	73.20	73.04	72.93	72.83

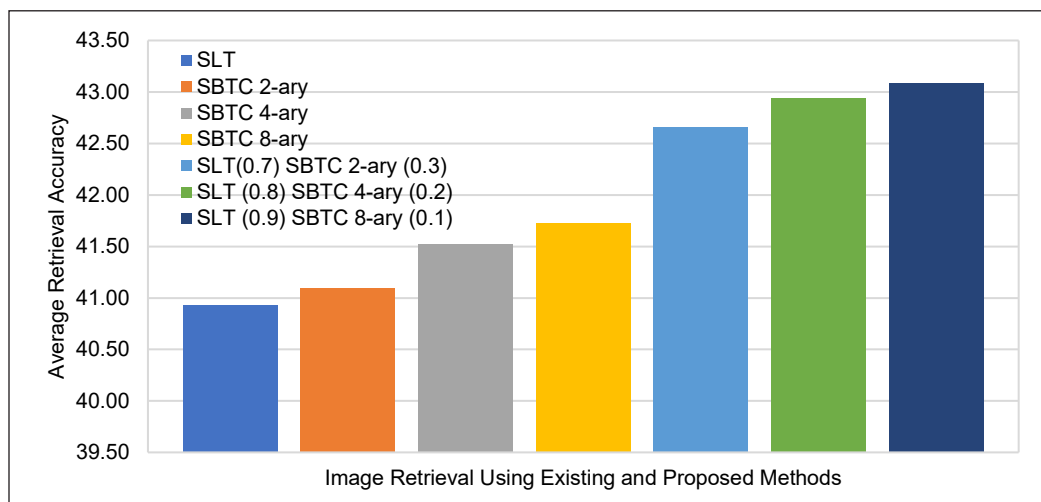


Figure 6. ARA using various existing and proposed IR methods (AWang dataset)

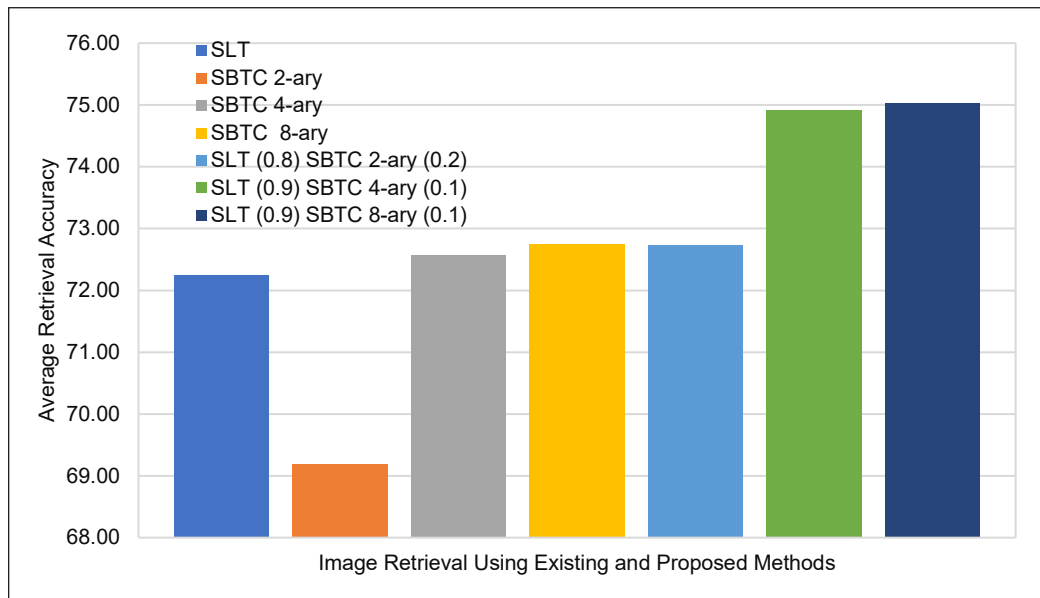


Figure 7. ARA using various existing and proposed IR methods (MCOIL dataset)

Statistical Significance

For statistical validation of obtained results, the proposed IR using weighted SLT and SBTC 8-ary feature fusion is compared with existing methods using a 2-variable t-Test, assuming equal variance is defined as:

H0: There is no significant difference between IR accuracy using weighted SLT and SBTC 8-ary and existing methods.

Ha: There is a significant difference between IR accuracy using weighted SLT and SBTC 8-ary and existing methods.

The obtained t-Stat, t-Critical, and P-value are given in Table 9. For the proposed method, when compared with the existing SLT method, the p-value for 2-tail is less than $\alpha(0.05)$, rejecting the null hypotheses (H0) and proving that the proposed weighted SLT (0.9 weight) and SBTC 8-ary (0.1 weight) method is statistically significant than the existing method.

Table 9
Statistical validation of proposed IR techniques

Parameters	SLT: 0.9	SLT: 0.8	SLT: 0.7	SLT: 0.6	SLT: 0.5	SLT: 0.4	SLT: 0.3	SLT: 0.2	SLT: 0.1
	SBTC: 0.1	SBTC: 0.2	SBTC: 0.3	SBTC: 0.4	SBTC: 0.5	SBTC: 0.6	SBTC: 0.7	SBTC: 0.8	SBTC: 0.9
	Mean	63.70	63.18	62.82	62.54	62.34	62.17	62.02	61.82
t Stat	-2.01	-1.46	-1.15	-0.95	-0.80	-0.68	-0.58	-0.51	-0.45
P(T<=t) two-tail	0.05	0.15	0.26	0.35	0.43	0.50	0.57	0.61	0.66
t Critical two-tail	2.04	2.04	2.04	2.04	2.04	2.04	2.04	2.04	2.04

CONCLUSION

The research paper has presented the fusion-based IR technique using weighted features of Sauvola local thresholding and the SBTC technique. The proposed method is tested with two different standard datasets, viz. AWang and MCOIL. The introduced IR using feature fusion of SLT and SBTC techniques has surpassed the performance in terms of average retrieval accuracy of the existing methods. It has revealed the statistical significance of improved IR. Results show that the proposed technique with SBTC 8-ary with 0.1 weight and SLT with 0.9 weight feature fusion gives better ARA than all the studied methods across the datasets considered.

In the future, it will be interesting to explore using various color spaces for feature extraction using the proposed method in IR. Future work can use various similarity metrics in addition to the currently used mean square error like Euclidian distance, cosine distance, and city block distance can be explored.

ACKNOWLEDGEMENT

The authors appreciate the cooperation of the Pimpri Chinchwad College of Engineering, India, in completing this work.

REFERENCES

- Abdel-Hakim, A. E., & Farag, A. A. (2006, June 17-22). *CSIFT: A SIFT descriptor with color invariant characteristics*. [Paper presentation]. 2006 IEEE Computer Society Conference on Computer Vision and Pattern Recognition (CVPR'06), New York, USA. <https://doi.org/10.1109/CVPR.2006.95>
- Alahi, A., Ortiz, R., & Vandergheynst, P. (2012, June 16-21). *FREAK: Fast retina keypoint*. [Paper presentation]. 2012 IEEE Conference on Computer Vision and Pattern Recognition, Providence, USA. <https://doi.org/10.1109/CVPR.2012.6247715>
- Alhassan, A. K., & Alfaki, A. A. (2017, January 16-18). *Color and texture fusion-based method for content-based image retrieval*. [Paper presentation]. 2017 International Conference on Communication, Control, Computing and Electronics Engineering (ICCCCEE), Khartoum, Sudan. <https://doi.org/10.1109/ICCCCEE.2017.7867649>
- Alkhawiani, M., Elmogy, M., & Elbakry, H. (2015). Content-based image retrieval using local features descriptors and bag-of-visual words. *International Journal of Advanced Computer Science and Applications*, 6(9), 212-219. <https://doi.org/10.14569/IJACSA.2015.060929>
- Arandjelovic, R., & Zisserman, A. (2012, June 16-21). *Three things everyone should know to improve object retrieval*. [Paper presentation]. 2012 IEEE Conference on Computer Vision and Pattern Recognition, Providence, USA. <https://doi.org/10.1109/CVPR.2012.6248018>
- Baji, F., & Mocanu, M. (2018). Chain code approach for shape based image retrieval. *Indian Journal of Science and Technology*, 11(3), 1-17. <https://doi.org/10.17485/ijst/2018/v11i3/119998>

- Bataineh, B., Abdullah, S. N. H. S., Omar, K., & Faidzul, M. (2011). Adaptive thresholding methods for documents image binarization. In J. F. Martinez-Trinidad, J. A. Carrasco-Oschoa, C. B. Y. Brants & E. R. Hancock (Eds.), *Pattern recognition* (pp. 230-239). Springer. https://doi.org/10.1007/978-3-642-21587-2_25
- Bay, H., Tuytelaars, T., & Van Gool, L. (2006). SURF: Speeded up robust features. In A. Leonardis, H. Bischof & A. Pinz (Eds.), *Computer vision ECCV 2006* (pp. 404-417). Springer. https://doi.org/10.1007/11744023_32
- Calonder, M., Lepetit, V., Strecha, C., & Fua, P. (2010). BRIEF: Binary robust independent elementary features. In K. Daniilidis, P. Maragos & N. Paragios (Eds.), *Computer vision ECCV 2010* (pp. 778-792). Springer. https://doi.org/10.1007/978-3-642-15561-1_56
- Cao, J., Huang, Y., Dai, Q., & Ling, W. K. (2021). Unsupervised trademark retrieval method based on attention mechanism. *Sensors*, 21(5), Article 1894. <https://doi.org/10.3390/s21051894>
- Chen, Y. H., Chang, C. C., Lin, C. C., & Hsu, C. Y. (2018). Content-based color image retrieval using block truncation coding based on binary ant colony optimization. *Symmetry*, 11(1), Article 21. <https://doi.org/10.3390/sym11010021>
- Cheung, W., & Hamarneh, G. (2007, April 12-15). *N-SIFT: N-dimensional scale invariant feature transform for matching medical images*. [Paper presentation]. 2007 4th IEEE International Symposium on Biomedical Imaging: From Nano to Macro, Arlington, USA. <https://doi.org/10.1109/ISBI.2007.356953>
- Dewan, J. H., & Thepade, S. D. (2021, March 5-7). *Fusion based image retrieval using haralick moments and TSBTC features*. [Paper presentation]. 2021 International Conference on Emerging Smart Computing and Informatics (ESCI), Pune, India. <https://doi.org/10.1109/ESCI50559.2021.9396833>
- Dhotre, D. R., & Bamnote, G. R. (2017, September 22-24). Multilevel haar wavelet transform and histogram usage in content based image retrieval system. [Paper presentation]. 2017 International Conference on Vision, Image and Signal Processing (ICVISP), Osaka, Japan. <https://doi.org/10.1109/ICVISP.2017.34>
- Du, A., Wang, L., & Qin, J. (2019). Image retrieval based on colour and improved NMI texture features. *Automatika: Časopis Za Automatiku, Mjerenje, Elektroniku, Računarstvo I Komunikacije*, 60(4), 491-499. <https://doi.org/10.1080/00051144.2019.1645977>
- Guo, J. M., & Liu, Y. F. (2014). Improved block truncation coding using optimized dot diffusion. *IEEE Transactions on Image Processing*, 23(3), 1269-1275. <https://doi.org/10.1109/TIP.2013.2257812>
- Guo, J. M., & Prasetyo, H. (2015). Content-based image retrieval using features extracted from halftoning-based block truncation coding. *IEEE Transactions on Image Processing*, 24(3), 1010-1024. <https://doi.org/10.1109/TIP.2014.2372619>
- Guo, J. M., Prasetyo, H., & Chen, J. H. (2015). Content-based image retrieval using error diffusion block truncation coding features. *IEEE Transactions on Circuits and Systems for Video Technology*, 25(3), 466-481. <https://doi.org/10.1109/TCSVT.2014.2358011>
- Guo, J. M., Prasetyo, H., & Wang, N. J. (2015). Effective image retrieval system using dot-diffused block truncation coding features. *IEEE Transactions on Multimedia*, 17(9), 1576-1590. <https://doi.org/10.1109/TMM.2015.2449234>

- Hadjadj, Z., Meziane, A., Cherfa, Y., Cheriet, M., & Setitria, I. (2016). ISauvola: Improved sauvola's algorithm for document image binarization. In A. Campilho & F. Karray (Eds.), *Image Analysis and Recognition* (pp. 737-745). https://doi.org/10.1007/978-3-319-41501-7_82
- Han, J., & Ma, K. K. (2002). Fuzzy color histogram and its use in color image retrieval. *IEEE Transactions on Image Processing*, 11(8), 944-952. <https://doi.org/10.1109/TIP.2002.801585>
- Haralick, R. M., Shanmugam, K., & Dinstein, I. (1973). Textural features for image classification. *IEEE Transactions on Systems, Man, and Cybernetics*, 6(SMC-3), 610-621. <https://doi.org/10.1109/TSMC.1973.4309314>
- Harris, C., & Stephens, M. (1988). A combined corner and edge detector. *Alvey Vision Conference*, 15(50), 147-151.
- Hua, J. Z., Liu, G. H., & Song, S. X. (2019). Content-based image retrieval using color volume histograms. *International Journal of Pattern Recognition and Artificial Intelligence*, 33(11), Article 1940010. <https://doi.org/10.1142/S021800141940010X>
- Huang, J., Kumar, S. R., Mitra, M., Zhu, W. J., & Rabih, R. (1997, June 17-19). *Image indexing using color correlograms*. [Paper presentation]. Proceedings of IEEE Computer Society Conference on Computer Vision and Pattern Recognition, Puerto Rico, USA. <https://doi.org/10.1109/CVPR.1997.609412>
- Jabeen, S., Mehmood, Z., Mahmood, T., Saba, T., Rehman, A., & Mahmood, M. T. (2018). An effective content-based image retrieval technique for image visual representation based on the bag-of-visual-words model. *PloS One*, 13(4), Article e0194526. <https://doi.org/10.1371/journal.pone.0194526>
- Ji, Y., Wang, W., Lv, Y., & Zhou, W. (2020). Research on fabric image retrieval method based on multi-feature layered fusionon. *Journal of Physics: Conference Series*, 1549(5), Article 052038. <https://doi.org/10.1088/1742-6596/1549/5/052038>
- Kayhan, N., & Fekri-Ershad, S. (2021). Content based image retrieval based on weighted fusion of texture and color features derived from modified local binary patterns and local neighborhood difference patterns. *Multimedia Tools and Applications*, 80(21-23), 32763-32790. <https://doi.org/10.1007/s11042-021-11217-z>
- Ke, Y., & Sukthankar, R. (2004, June 27 - July 2). *PCA-SIFT: A more distinctive representation for local image descriptors*. [Paper presentation]. Proceedings of the 2004 IEEE Computer Society Conference on Computer Vision and Pattern Recognition, 2004. CVPR 2004., 2, Washington, USA. <https://doi.org/10.1109/CVPR.2004.1315206>
- Latif, A., Rasheed, A., Sajid, U., Ahmed, J., Ali, N., Ratyal, N. I., Zafar, B., Dar, S. H., Sajid, M., & Khalil, T. (2019). Content-based image retrieval and feature extraction: A comprehensive review. *Mathematical Problems in Engineering*, 2019, Article 9658350. <https://doi.org/10.1155/2019/9658350>
- Lazzara, G., & Géraud, T. (2014). Efficient multiscale Sauvola's binarization. *International Journal on Document Analysis and Recognition (IJDAR)*, 17(2), 105-123. <https://doi.org/10.1007/s10032-013-0209-0>
- Lee, J., Jin, R., Jain, A., & Tong, W. (2012). Image retrieval in forensics: Tattoo image database application. *IEEE Multimedia*, 19(1), 40-49. <https://doi.org/10.1109/MMUL.2011.59>
- Leutenegger, S., Chli, M., & Siegwart, R. Y. (2011, November 6-13). *BRISK: Binary Robust invariant scalable keypoints*. [Paper presentation]. 2011 International Conference on Computer Vision, Barcelona, Spain. <https://doi.org/10.1109/ICCV.2011.6126542>

- Li, J., & Wang, J. Z. (2003). Automatic linguistic indexing of pictures by a statistical modeling approach. *IEEE Transactions on Pattern Analysis and Machine Intelligence*, 25(9), 1075–1088. <https://doi.org/10.1109/TPAMI.2003.1227984>
- Loupia, E., Sebe, N., Bres, S., & Jolion, J. M. (2000, September 10-13). *Wavelet-based salient points for image retrieval*. [Paper presentation]. Proceedings 2000 International Conference on Image Processing (Cat. No.00CH37101), Vancouver, Canada. <https://doi.org/10.1109/ICIP.2000.899469>
- Lowe, D. G. (2004). Distinctive image features from scale-invariant keypoints. *International Journal of Computer Vision*, 60(2), 91-110. <https://doi.org/10.1023/B:VISI.0000029664.99615.94>
- Manjunath, B. S., & Ma, W. Y. (1996). Texture features for browsing and retrieval of image data. *IEEE Transactions on Pattern Analysis and Machine Intelligence*, 18(8), 837-842. <https://doi.org/10.1109/34.531803>
- Matas, J., Chum, O., Urban, M., & Pajdla, T. (2004). Robust wide-baseline stereo from maximally stable extremal regions. *Image and Vision Computing*, 22(10), 761-767. <https://doi.org/https://doi.org/10.1016/j.imavis.2004.02.006>
- Mehmood, Z., Abbas, F., Mahmood, T., Javid, M. A., Rehman, A., & Nawaz, T. (2018). Content-based image retrieval based on visual words fusion versus features fusion of local and global features. *Arabian Journal for Science and Engineering*, 43(12), 7265-7284. <https://doi.org/10.1007/s13369-018-3062-0>
- Mikolajczyk, K., & Schmid, C. (2001, July 7-14). *Indexing based on scale invariant interest points*. [Paper presentation]. Proceedings Eighth IEEE International Conference on Computer Vision. ICCV 2001, Vancouver, Canada. <https://doi.org/10.1109/ICCV.2001.937561>
- Mikolajczyk, K., & Schmid, C. (2002). An affine invariant interest point detector. In A. Heyden, G. Sparr, M. Nielsen & P. Johansen (Eds.), *Computer vision – ECCV 2002* (pp. 128-142). Springer. https://doi.org/10.1007/3-540-47969-4_9
- Mistry, Y., Ingole, D. T., & Ingole, M. D. (2016, April 28-30). *Efficient content based image retrieval using transform and spatial feature level fusion*. [Paper presentation]. 2016 2nd International Conference on Control, Automation and Robotics (ICCAR), Hong Kong, China. <https://doi.org/10.1109/ICCAR.2016.7486744>
- Müller, H. (2020, June 8-11). *Medical image retrieval: applications and resources*. [Paper presentation]. ICMR '20: Proceedings of the 2020 International Conference on Multimedia Retrieval, New York, USA. <https://doi.org/10.1145/3372278.3390668>
- Murala, S., Maheshwari, R. P., & Balasubramanian, R. (2012a). Local tetra patterns: A new feature descriptor for content-based image retrieval. *IEEE Transactions on Image Processing*, 21(5), 2874-2886. <https://doi.org/10.1109/TIP.2012.2188809>
- Murala, S., Maheshwari, R. P., & Balasubramanian, R. (2012b). Directional local extrema patterns: A new descriptor for content based image retrieval. *International Journal of Multimedia Information Retrieval*, 1(3), 191-203. <https://doi.org/10.1007/s13735-012-0008-2>
- Nene, S. A., Nayar, S. K., & Murase, H. (n.d.). *Columbia Object Image Library (COIL-20)*. Retrieved July 20, 2019, from http://www.cs.columbia.edu/CAVE/publications/pdfs/Nene_TR96.pdf

- Ojala, T., Pietikäinen, M., & Harwood, D. (1996). A comparative study of texture measures with classification based on featured distributions. *Pattern Recognition*, 29(1), 51-59. [https://doi.org/10.1016/0031-3203\(95\)00067-4](https://doi.org/10.1016/0031-3203(95)00067-4)
- Pass, G., Zabih, R., & Miller, J. (1996, November 18-22). *Comparing images using color coherence vectors*. [Paper presentation]. MM96: The Fourth ACM International Multimedia Conference, Massachusetts, USA. <https://doi.org/10.1145/244130.244148>
- Rosten, E., & Drummond, T. (2006). Machine learning for high-speed corner detection. In A. Leonardis, H. Bischof, & A. Pinz (Eds.), *Computer vision - ECCV 2006* (pp. 430-443). Springer. https://doi.org/10.1007/11744023_34
- Rublee, E., Rabaud, V., Konolige, K., & Bradski, G. (2011, November 6-13). *ORB: An efficient alternative to SIFT or SURF*. [Paper presentation]. 2011 International Conference on Computer Vision, Barcelona, Spain. <https://doi.org/10.1109/ICCV.2011.6126544>
- Sauvola, J., & Pietikäinen, M. (2000). Adaptive document image binarization. *Pattern Recognition*, 33(2), 225-236. [https://doi.org/10.1016/S0031-3203\(99\)00055-2](https://doi.org/10.1016/S0031-3203(99)00055-2)
- Shao, H., Wu, Y., Cui, W., & Zhang, J. (2008, November 18-21). *Image retrieval based on MPEG-7 dominant color descriptor*. [Paper presentation]. 2008 The 9th International Conference for Young Computer Scientists, Hunan China. <https://doi.org/10.1109/ICYCS.2008.89>
- Shi, J., & Tomasi. (1994, June 21-23). *Good features to track*. [Paper presentation]. Proceedings of IEEE Conference on Computer Vision and Pattern Recognition, Seattle, USA. <https://doi.org/10.1109/CVPR.1994.323794>
- Shifa, A., Afgan, M. S., Asghar, M. N., Fleury, M., Memon, I., Abdullah, S., & Rasheed, N. (2018). Joint crypto-stego scheme for enhanced image protection with nearest-centroid clustering. *IEEE Access*, 6, 16189-16206. <https://doi.org/10.1109/ACCESS.2018.2815037>
- Singh, V. P., & Srivastava, R. (2018). Effective image retrieval based on hybrid features with weighted similarity measure and query image classification. *International Journal of Computational Vision and Robotics*, 8(2), Article 98. <https://doi.org/10.1504/IJCVR.2018.091979>
- Smith, S. M., & Brady, J. M. (1997). SUSAN-A new approach to low level image processing. *International Journal of Computer Vision*, 23(1), 45-78. <https://doi.org/10.1023/A:1007963824710>
- Srivastava, P., & Khare, A. (2018). Utilizing multiscale local binary pattern for content-based image retrieval. *Multimedia Tools and Applications*, 77(10), 12377-12403. <https://doi.org/10.1007/s11042-017-4894-4>
- Sumana, I. J., Islam, M. M., Zhang, D., & Lu, G. (2008, October 8-10). *Content based image retrieval using curvelet transform*. [Paper presentation]. 2008 IEEE 10th Workshop on Multimedia Signal Processing, Cairns, Australia. <https://doi.org/10.1109/MMSP.2008.4665041>
- Sun, J., & Wu, X. (2006, December 18-20). *Chain code distribution-based image retrieval*. [Paper presentation]. 2006 International Conference on Intelligent Information Hiding and Multimedia, California, USA . <https://doi.org/10.1109/IIH-MSP.2006.264973>
- Tamura, H., Mori, S., & Yamawaki, T. (1978). Textural features corresponding to visual perception. *IEEE Transactions on Systems, Man, and Cybernetics*, 8(6), 460-473. <https://doi.org/10.1109/TSMC.1978.4309999>

- Tarawneh, A. S., Hassanat, A. B. A., Celik, C., Chetverikov, D., Rahman, M. S., & Verma, C. (2018). *Deep Face Image Retrieval: A Comparative Study with Dictionary Learning*. ArXiv. <http://arxiv.org/abs/1812.05490>
- Tunio, M. H., Memon, I., Mallah, G. A., Shaikh, N. A., Shaikh, R. A., & Magsi, Y. (2020, February 8-9). *Automation of traffic control system using image morphological operations*. [Paper presentation]. 2020 International Conference on Information Science and Communication Technology (ICISCT), Karachi, India. <https://doi.org/10.1109/ICISCT49550.2020.9080051>
- Van De Sande, K., Gevers, T., & Snoek, C. (2010). Evaluating color descriptors for object and scene recognition. *IEEE Transactions on Pattern Analysis and Machine Intelligence*, 32(9), 1582-1596. <https://doi.org/10.1109/TPAMI.2009.154>
- Varish, N., Pal, A. K., Hassan, R., Hasan, M. K., Khan, A., Parveen, N., Banerjee, D., Pellakuri, V., Haqis, A. U., & Memon, I. (2020). Image retrieval scheme using quantized bins of color image components and adaptive tetrolet transform. *IEEE Access*, 8, 117639-117665. <https://doi.org/10.1109/ACCESS.2020.3003911>
- Wang, J., Wang, L., Liu, X., Ren, Y., & Yuan, Y. (2018). Color-based image retrieval using proximity space theory. *Algorithms*, 11(8), Article 115. <https://doi.org/10.3390/a11080115>
- Wang, J. Z., Li, J., & Wiederhold, G. (2001). SIMPLIcity: Semantics-sensitive integrated matching for picture libraries. *IEEE Transactions on Pattern Analysis and Machine Intelligence*, 23(9), 947–963. <https://doi.org/10.1109/34.955109>
- Xiaoling, W., & Kanglin, X. (2004, September 16). *A novel direction chain code-based image retrieval*. [Paper presentation]. The Fourth International Conference OnComputer and Information Technology, 2004. CIT '04., Wuhan, China. <https://doi.org/10.1109/CIT.2004.1357195>
- Yang, Z., Ge, Y., Huang, Z., & Xiong, C. (2021, March 26-28). *Supervised hashing with kernel based on feature fusion for remote sensing image retrieval*. [Paper presentation]. 2021 IEEE 2nd International Conference on Big Data, Artificial Intelligence and Internet of Things Engineering (ICBAIE), Nanchang, China. <https://doi.org/10.1109/ICBAIE52039.2021.9389931>
- Yu, G., & Morel, J. M. (2011). ASIFT: An algorithm for fully affine invariant comparison. *Image Processing On Line*, 1, 11-38. <https://doi.org/10.5201/ipl.2011.my-asift>
- Yu, J., Qin, Z., Wan, T., & Zhang, X. (2013). Feature integration analysis of bag-of-features model for image retrieval. *Neurocomputing*, 120, 355-364. <https://doi.org/10.1016/j.neucom.2012.08.061>
- Zhang, B., Gao, Y., Zhao, S., & Liu, J. (2010). Local derivative pattern versus local binary pattern: Face recognition with high-order local pattern descriptor. *IEEE Transactions on Image Processing*, 19(2), 533-544. <https://doi.org/10.1109/TIP.2009.2035882>
- Zhang, S., Tian, Q., Lu, K., Huang, Q., & Gao, W. (2013). Edge-SIFT: Discriminative binary descriptor for scalable partial-duplicate mobile search. *IEEE Transactions on Image Processing*, 22(7), 2889-2902. <https://doi.org/10.1109/TIP.2013.2251650>